Chemical Engineering Journal 147 (2009) 405–411

Contents lists available at ScienceDirect

Chemical Engineering Journal

journal homepage: www.elsevier.com/locate/cej

Formation of TiB_2–Al_2O_3 and NbB_2–Al_2O_3 composites by combustion synthesis involving thermite reactions

C.L. Yeh [a,*], R.F. Li [b]

[a] Department of Aerospace and Systems Engineering, Feng Chia University, Taichung 40724, Taiwan
[b] Department of Mechanical and Automation Engineering, Da-Yeh University, Changhua 51591, Taiwan

ARTICLE INFO

Article history:
Received 10 September 2008
Received in revised form 15 December 2008
Accepted 2 January 2009

Keywords:
Self-propagating high-temperature synthesis
Thermite reactions
TiB_2–Al_2O_3 Composite
NbB_2–Al_2O_3 Composite
Flame-front velocity

ABSTRACT

Preparation of TiB_2–Al_2O_3 and NbB_2–Al_2O_3 in situ composites with a broad range of phase composition was conducted by self-propagating high-temperature synthesis (SHS) involving thermite reactions of different types. Thermite mixtures of Al–TiO_2 and Al–TiO_2–B_2O_3 were incorporated with the Ti–B combustion system to produce the composites of TiB_2–Al_2O_3, within which the increase of the thermite mixture for a higher content of Al_2O_3 decreased the reaction temperature and combustion wave velocity. This implies that the thermite reaction of Al with TiO_2 reduces the exothermicity of the overall SHS process. In the synthesis of NbB_2–Al_2O_3 composite, two thermite mixtures of Al–Nb_2O_5 and Al–Nb_2O_5–B_2O_3 were added to the Nb–B combustion system and both of which were found to increase the combustion temperature and propagation rate of the flame front. This is due to the highly exothermic nature of the thermite reaction between Al and Nb_2O_5. For both kinds of composites, it was found that adoption of B_2O_3 as one of the thermite reagents improved the product formation effectively. The XRD analysis shows that the final products composed of no more than TiB_2 and Al_2O_3 are obtained from the powder compacts containing the thermite mixture of Al–TiO_2–B_2O_3. On formation of the NbB_2–Al_2O_3 composite, NbB_2 is identified as the major boride phase in the products involving the thermite reactions of Al–Nb_2O_5–B_2O_3, while Nb_3B_4 dominates in the case of using Al and Nb_2O_5 as the thermite reagents.

1. Introduction

Transition metal diborides like TiB_2 and NbB_2 possess many superior properties, such as high melting points, high hardness, good thermal and electrical conductivity, excellent wear and corrosion resistance, and chemical stability [1–3]. Moreover, addition of Al_2O_3 to these metal borides further improves their fracture toughness, flexural strength, and impact resistance, which renders the Al_2O_3-reinforced boride composites a promising candidate for a variety of the applications including cutting tools, wear-resistant parts, and high-temperature structural materials [1,3–5].

Among various reaction-based synthesis methods, combustion synthesis in the mode of self-propagating high-temperature synthesis (SHS) is particularly attractive, on account of its advantages of low energy requirement, short processing time, simplicity of facilities, and formation of high-purity products [6–9]. The SHS technique has been extensively applied to produce a great number of advanced materials such as borides, carbides, nitrides, silicides, and intermetallics such as aluminides [6–9]. When incorporated with thermite reactions based on Al as the reducing agent, the SHS approach represents an in situ procedure for preparing ceramic, intermetallic, and metal matrix composites reinforced by Al_2O_3, because such thermite reactions are highly exothermic and produce a stable oxide Al_2O_3 [10–15]. By using the powder compact composed of Al, ZrO_2, and B_2O_3 as the raw materials, Mishra et al. [4] successfully fabricated the ZrB_2–Al_2O_3 composite through the SHS process. Similarly, an in situ composite with TiB_2:Al_2O_3 = 3:5 was produced from the test specimen consisting of $3TiO_2$–$3B_2O_3$–10Al [11]. The reaction system of Ti–Al–TiO_2 was employed under different starting stoichiometries to prepare the TiAl–Al_2O_3 composites [12] and Ti–Al_2O_3 cermets [13]. Vallauri et al. [14] applied the SHS route involving the thermite reagent of TiO_2 reduced by Al, Mg, and Zr to fabricate TiC–TiB_2-based composites reinforced by different metallic oxides including Al_2O_3, MgO, and ZrO_2. For direct formation of dense TiC–Al_2O_3–Al composites, Hu et al. [15] conducted the field-activated combustion synthesis to overcome thermodynamic limitations of the $3TiO_2$–3C–$(4+x)$Al system with $x \geq 10$. One additional benefit from combining thermite-based displacement reactions with conventional combustion synthesis is the cost savings, since the metallic oxides like TiO_2, B_2O_3, and ZrO_2 are considerably less expensive than elemental titanium, boron, and zirconium.

The objective of this study is to investigate formation of the TiB_2–Al_2O_3 and NbB_2–Al_2O_3 in situ composites with a broad range

* Corresponding author. Tel.: +886 4 24517250x3963; fax: +886 4 24510862.
E-mail address: clyeh@fcu.edu.tw (C.L. Yeh).

1385-8947/$ – see front matter © 2009 Elsevier B.V. All rights reserved.
doi:10.1016/j.cej.2009.01.007

of phase composition by the SHS process involving thermite reactions of different types. On formation of the TiB_2–Al_2O_3 composite, two thermite mixtures, Al–TiO_2 and Al–TiO_2–B_2O_3, were added to the Ti–B elemental combustion system and their resulting effects were compared. Similarly, thermite mixtures of Al–Nb_2O_5 and Al–Nb_2O_5–B_2O_3 were adopted for the synthesis of the NbB_2–Al_2O_3 composite, which has not been previously studied by combustion synthesis. In this study, the influence of the thermite reaction on the SHS process was explored in terms of the combustion sustainability, propagation rate of the reaction front, combustion temperature, and phase composition of the synthesized products.

2. Experimental methods of approach

The starting materials used in this study included four elemental powders: Ti (Strem Chemicals, <45 mm, 99% purity), Nb (Strem Chemicals, <45 mm, 99.8% purity), amorphous boron (Noah Technologies Corp., 1 mm, 92% purity), and Al (Showa Chemical Co., 10 mm, 99.9% purity). Additionally, three metallic oxides, TiO_2 (Showa Chemical Co., 0.2–0.4 mm, 99.9% purity), Nb_2O_5 (Strem Chemicals, <45 mm, 99.9% purity), and B_2O_3 (Strem Chemicals, <45 mm, 99.6% purity), were employed as the thermite reagents. Similar to typical amorphous boron, the major impurities in the boron specimen used in this study include magnesium (Mg) about 5.0%, water soluble boron (0.50%) and moisture (0.50%). The initial stoichiometry of the powder blend for the synthesis of the TiB_2–Al_2O_3 composite was prepared according to two different thermite mixtures involved in the SHS process and described in Reactions (1) and (2).

$$\left(1-\frac{5}{2}x\right)\mathrm{Ti}+2(1-x)\mathrm{B}+2x\mathrm{Al}+\frac{3}{2}x\mathrm{TiO_2}\rightarrow(1-x)\mathrm{TiB_2}+x\mathrm{Al_2O_3} \quad (1)$$

$$\left(1-\frac{8}{5}y\right)\mathrm{Ti}+2\left(1-\frac{8}{5}y\right)\mathrm{B}+2y\,\mathrm{Al}+\frac{3}{5}y\,\mathrm{TiO_2}+\frac{3}{5}y\mathrm{B_2O_3}\rightarrow(1-y)\,\mathrm{TiB_2}+y\,\mathrm{Al_2O_3} \quad (2)$$

where the stoichiometric parameters x and y represent the mole fraction of Al_2O_3 formed in the TiB_2–Al_2O_3 composite. The maximum value of x adopted in Reaction (1) was 0.35, because the reaction ceased to be self-propagating after ignition in the sample of $x = 0.4$, which signifies no elemental Ti included in the reactant mixture. The parameter y was varied from 0.2 to the upper limit of 0.625, under which the sample was composed of three thermite reagents Al, TiO_2, and B_2O_3.

When preparing the composite of NbB_2–Al_2O_3, the starting stoichiometry of the powder mixture was formulated as Reactions (3) and (4).

$$\left(1-\frac{11}{5}p\right)\mathrm{Nb}+2(1-p)\mathrm{B}+2p\mathrm{Al}+\frac{3}{5}p\mathrm{Nb_2O_5}\rightarrow(1-p)\mathrm{NbB_2}+p\mathrm{Al_2O_3} \quad (3)$$

$$\left(1-\frac{17}{11}q\right)\mathrm{Nb}+2\left(1-\frac{17}{11}q\right)\mathrm{B}+2q\mathrm{Al}+\frac{3}{11}q\mathrm{Nb_2O_5}+\frac{6}{11}q\mathrm{B_2O_3}\rightarrow(1-q)\mathrm{NbB_2}+q\mathrm{Al_2O_3} \quad (4)$$

where the parameters p and q stand for the mole fraction of Al_2O_3 formed in the NbB_2–Al_2O_3 composite. Samples of Reaction (3) were conducted with initial compositions up to the greatest extent of $p = 5/11$ (about 0.455), indicative of a test specimen without any elemental Nb. For the comparison purpose, the parameter q adopted in Reaction (4) ranged between 0.2 and 0.5.

The adiabatic combustion temperatures (T_{ad}) of Reactions (1)–(4) conducted in this study are calculated according to the following equation [16,17] with the thermochemical data from Ref. [18].

$$\Delta H+\int_{298}^{T_{ad}}\sum n_jC_p(P_j)dT+\sum_{298-T_{ad}}n_jL(P_j)=0 \quad (5)$$

where ΔH is the reaction enthalpy at 298 K, n_j the stoichiometric constant, C_p and L are the heat capacity and latent heat, and P_j refers to the product.

The constituent powders with designed stoichiometry were dry mixed in a ball mill and then cold-pressed into cylindrical samples with a diameter of 7 mm, a height of 12 mm, and a compaction density of 60% relative to the theoretical maximum density (TMD). The SHS experiment was performed in a stainless-steel windowed combustion chamber under an atmosphere of high-purity argon (99.99%). The propagation velocity of the combustion wave was measured by recording the whole combustion event with a color CCD video camera (Pulnix TMC-7) at 30 frames per second. The exposure time of each recorded image was set at 0.1 ms. To facilitate the accurate measurement of instantaneous locations of the combustion front, a beam splitter (Rolyn Optics), with a mirror characteristic of 75% transmission and 25% reflection, was used to optically superimpose a scale onto the image of the test sample. The superimposed scale image with a unit of mm is clearly seen on the left-hand side of each picture shown in Fig. 1. Details of the experimental setup and methods of measurement approach were reported elsewhere [19,20]. The microstructure of synthesized products was examined under a scanning electron microscope (Hitachi S-3000N), and phase composition was analyzed by an X-ray diffractometer (Shimadzu XRD-6000) with CuK_α radiation.

3. Results and discussion

3.1. Observation of combustion characteristics

Fig. 1a and b illustrates typical SHS sequences associated with formation of the TiB_2–Al_2O_3 and NbB_2–Al_2O_3 in situ composites, respectively. As observed from Fig. 1, a distinct combustion front forms upon ignition and propagates along the sample in a self-sustaining manner. It was also evident that the powder compact was subjected to significant elongation as the combustion wave progressed, resulting in the synthesized product with a porous structure. Because the volume expansion occurred on the burned portion of the sample compact, it had no effect on the measurement of the propagation velocity of the flame front. Formation of porous products is inherent in the SHS process. The pores or crevices could be produced by unbalanced diffusion between the reactant particles or by vaporization and expulsion of the volatile impurities due to high temperatures [21,22]. The expelled gases observed in Fig. 1 were most likely generated from vaporization of the low boiling point impurities (mainly Mg) in amorphous boron used in this study.

3.2. Measurement of flame-front propagation velocity

The propagation velocity (V_f) of the combustion front was determined from the recorded SHS images. Fig. 2 plots the flame-front velocity of the SHS process as a function of the Al_2O_3 content in the TiB_2–Al_2O_3 composites synthesized from the samples with two different thermite mixtures. When compared with those (over 40 mm/s) of the elemental SHS reaction producing monolithic TiB_2, the combustion wave velocity in the synthesis of TiB_2–Al_2O_3 composites is considerably lower and decreases with increasing Al_2O_3 content formed in the products. The decrease in flame-front veloc-

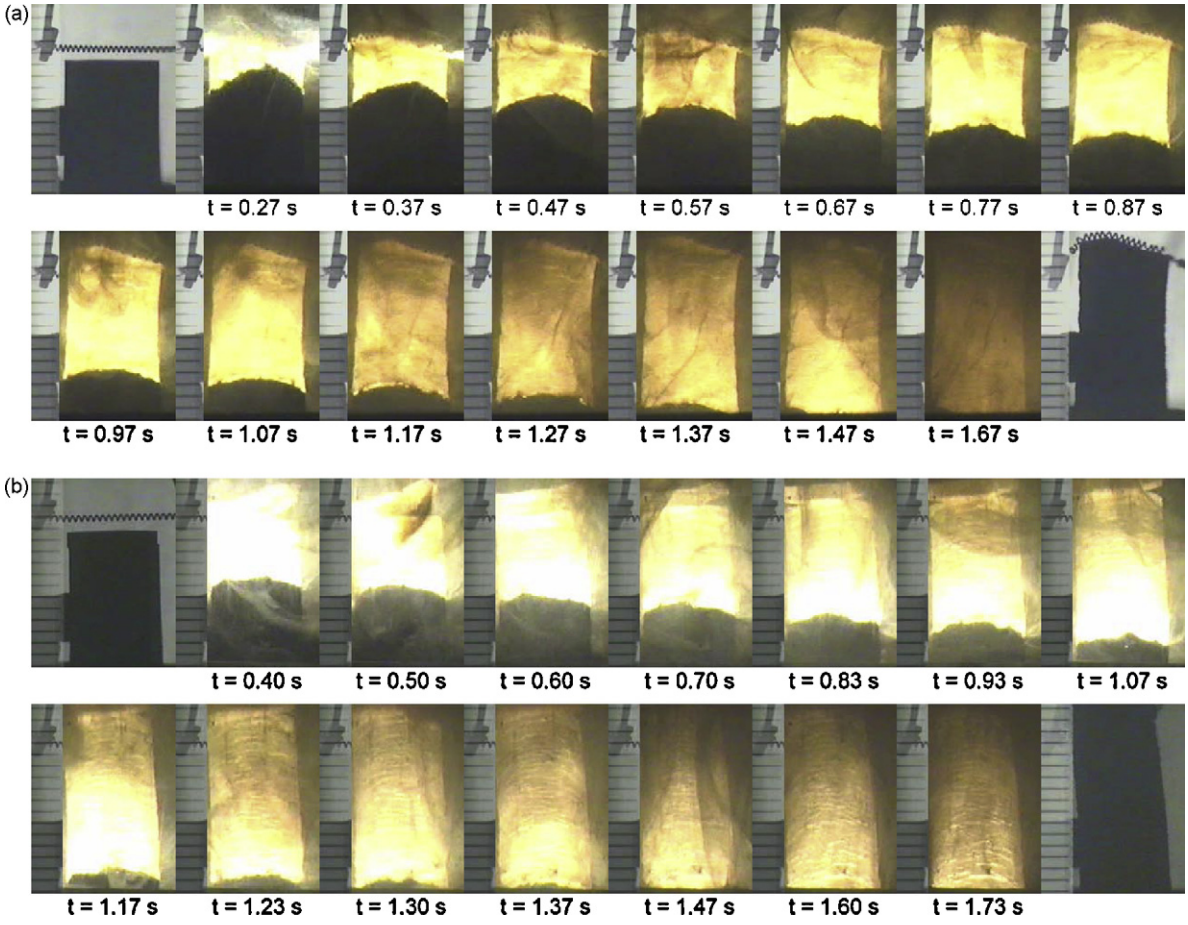

Fig. 1. Recorded images illustrating self-propagating combustion fronts along (a) a sample of Ti–B–Al–TiO_2–B_2O_3 based on Reaction (2) with $y = 0.45$ and (b) a sample of Nb–B–Al–Nb_2O_5–B_2O_3 based on Reaction (4) with $q = 0.3$.

ity is believed to be caused by reduced exothermicity of the overall synthesis reaction, in view of the fact that both the Al–TiO_2 and Al–TiO_2–B_2O_3 thermite systems yet releasing heat are less exothermic than the elemental reaction between Ti and B. Moreover, due to lack of sufficient thermal energy to sustain the synthesis reaction, combustion was found quenched in the sample based upon Reaction (1) with $x = 0.4$, under which no elemental Ti is employed and the powder compact contains B, Al, and TiO_2 only. This suggests that the elemental reaction between Ti and B plays a crucial role in triggering the thermite reaction of Al with TiO_2 in Reaction (1).

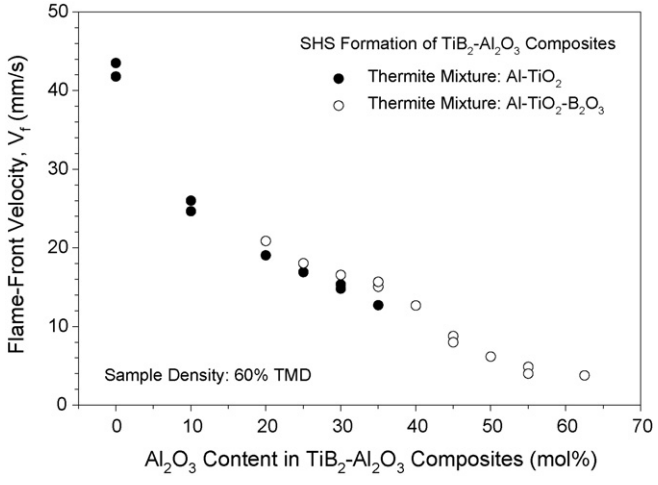

Fig. 2. Variation of flame-front velocity of SHS processes involving two different thermite mixtures with Al_2O_3 content formed in TiB_2–Al_2O_3 composites.

For the samples adopting the thermite mixture of Al–TiO_2–B_2O_3, Fig. 2 reveals a slightly greater speed of the combustion wave and a broader range of the composition that indicates better sustainability of the reaction. This might be due to formation of a molten B_2O_3 phase that improves contact between the reactant particles and thus facilitates the ignition and increases the reaction rate [10]. It is interesting to note that despite a relatively low speed of about 3.76 mm/s, self-sustaining combustion was achievable in the test specimen based upon Reaction (2) with $y = 0.625$, which means a sample composed only of Al, TiO_2, and B_2O_3 powders.

The flame-front propagation velocities measured from the samples for the preparation of NbB_2–Al_2O_3 composites are presented in Fig. 3. In contrast to formation of the TiB_2–Al_2O_3 composite, addition of either Al–Nb_2O_5 or Al–Nb_2O_5–B_2O_3 thermite mixture to the Nb–B elemental reaction accelerates the reaction front velocity significantly. As indicated in Fig. 3, the highest reaction front velocity up to 33 mm/s is observed in the sample containing the thermite mixture of Al–Nb_2O_5 with $p = 0.455$, within which the metallic oxide Nb_2O_5 serves as the only source of Nb. This implies that the thermite reaction of Al with Nb_2O_5 is sufficiently exothermic and has a great tendency to proceed. Fig. 3 also shows a lower flame-front velocity for the sample containing the thermite mixture of Al–Nb_2O_5–B_2O_3, mainly because the thermite reaction between Al and Nb_2O_5 is more exothermic than that of Al with B_2O_3 [10].

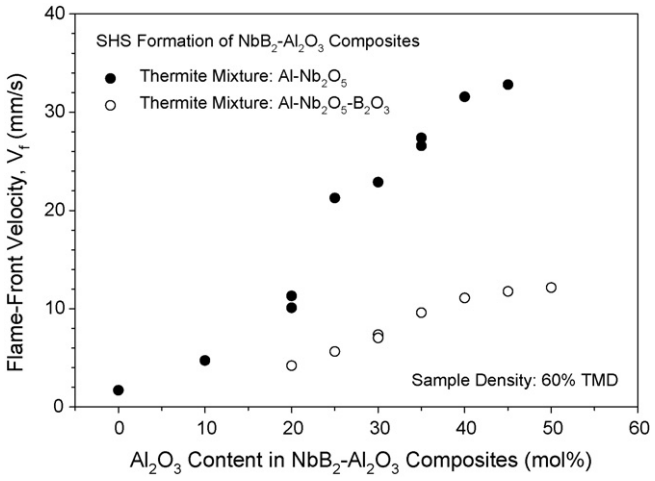

Fig. 3. Variation of flame-front velocity of SHS processes involving two different thermite mixtures with Al_2O_3 content formed in NbB_2–Al_2O_3 composites.

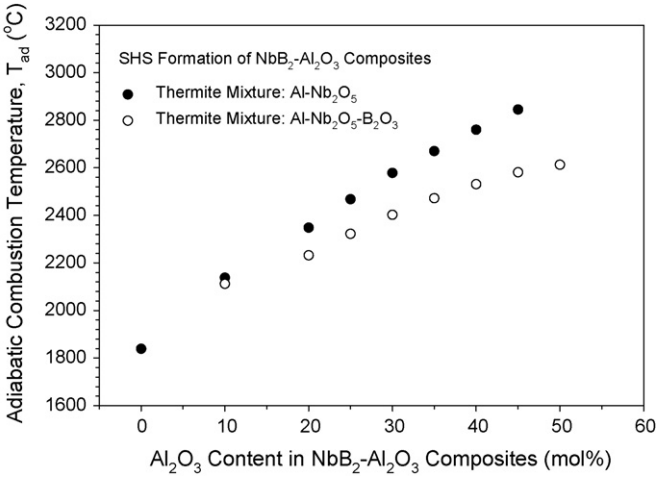

Fig. 5. Effect of Al_2O_3 content on adiabatic combustion temperatures associated with SHS formation of NbB_2–Al_2O_3 composites involving two different thermite mixtures.

3.3. Measurement of combustion temperature

Based upon Eq. (5), Fig. 4 shows the decrease in the calculated adiabatic temperature with increasing Al_2O_3 content in the TiB_2–Al_2O_3 composites, mainly because the elemental reaction of Ti with B is more exothermic than the displacement reaction within the thermite mixture. Additionally, on account of the higher heat of formation of B_2O_3 than TiO_2, the SHS processes involving the thermite mixture of Al–TiO_2–B_2O_3 exhibit higher adiabatic temperatures when compared with those using the Al–TiO_2 mixture.

For the synthesis of the NbB_2–Al_2O_3 composites, however, Fig. 5 reveals that the adiabatic combustion temperature increases with Al_2O_3 content. This is caused by the fact that the thermite reaction of Al with Nb_2O_5 and B_2O_3 is more energetic than the elemental reaction between Nb and B. Moreover, due to the higher heat of formation of Nb_2O_5 than B_2O_3, higher adiabatic temperatures were observed in the samples containing Al and Nb_2O_5 as the thermite reagents than those with an Al–Nb_2O_5–B_2O_3 mixture. It is useful to note that variations of the flame-front propagation velocity observed in Figs. 2 and 3 with the Al_2O_3 content of the product and the composition of the thermite mixture agree reasonably with those of the adiabatic combustion temperature presented in Figs. 4 and 5.

Fig. 6 depicts measured combustion temperature profiles associated with the formation of TiB_2–Al_2O_3 and NbB_2–Al_2O_3 composites containing different Al_2O_3 contents from the SHS processes involving the thermite reactions of Al–TiO_2 and Al–Nb_2O_5, respectively. The abrupt rise in the temperature profile represents rapid arrival of the combustion wave and the peak value signifies the reaction front temperature. After the passage of the flame front, an appreciable decrease in temperature is a consequence of heat losses to the surroundings. Fig. 6 shows that for the production of TiB_2–Al_2O_3 composites, the reaction front temperature decreases from 1690 to 1500 °C as the extent of the thermite reaction augments for increasing the Al_2O_3 content from 20 to 35 mol%, which suggests a decrease in the reaction exothermicity with increasing proportion of the thermite reaction in the overall SHS reaction. On the other hand, Fig. 6 reveals an increase in the reaction front temperature with Al_2O_3 content formed in the NbB_2–Al_2O_3 composites, which provides evidence that the exothermicity of the overall synthesis process increases with the degree of the Al–Nb_2O_5 thermite reaction involved.

For the powder compacts with different thermite reactants, as shown in Fig. 7, comparable combustion temperatures were detected under the conditions of producing the TiB_2–35 mol% Al_2O_3 composites. However, for the formation of NbB_2–40 mol% Al_2O_3

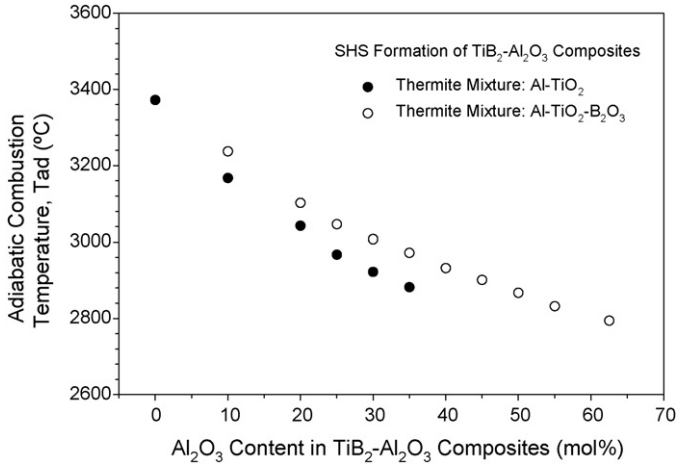

Fig. 4. Effect of Al_2O_3 content on adiabatic combustion temperatures associated with SHS formation of TiB_2–Al_2O_3 composites involving two different thermite mixtures.

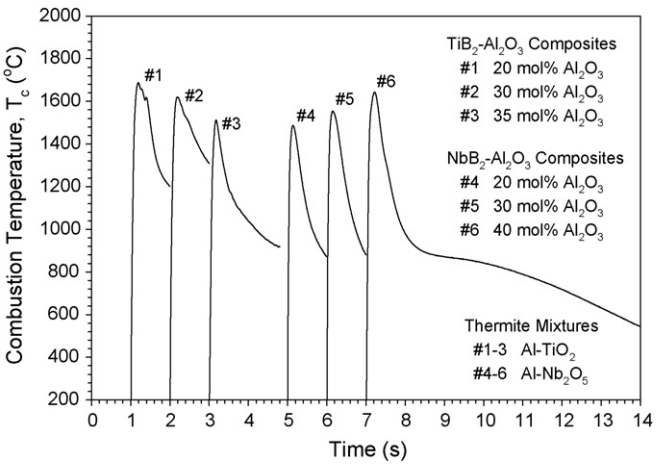

Fig. 6. Effects of Al_2O_3 content on measured combustion temperatures associated with formation of TiB_2–Al_2O_3 and NbB_2–Al_2O_3 composites by SHS processes involving thermite mixtures of Al–TiO_2 and Al–Nb_2O_5, respectively.

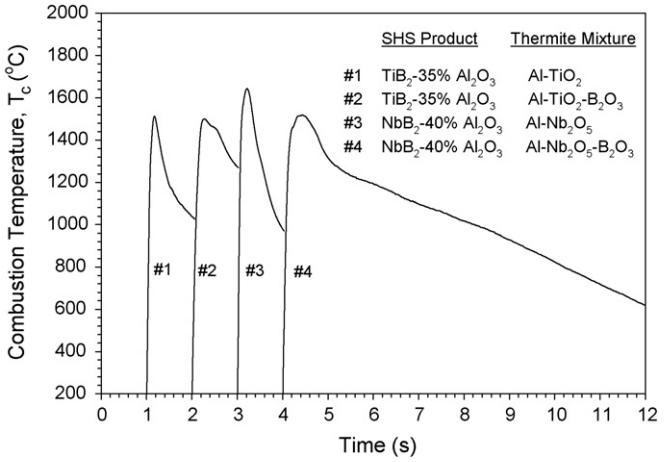

Fig. 7. Effects of different thermite mixtures on measured combustion temperatures associated with formation of TiB_2–Al_2O_3 and NbB_2–Al_2O_3 composites by SHS processes.

composites, it was found a higher combustion temperature for the sample compact containing Al and Nb_2O_5 as the thermite reagents than that adopting Al, Nb_2O_5, and B_2O_3. Even though the measured combustion temperatures are appreciably lower than the adiabatic values due largely to the heat loss to the surroundings, variations of the measured combustion temperature with experimental variables are in a manner consistent with those under an adiabatic condition.

3.4. Composition and morphology analysis of combustion products

Fig. 8a and b shows typical XRD patterns of the synthesized products from the samples of Reactions (1) and (2), respectively. In the case of using Al and TiO_2 as the thermite reagents, Fig. 8a indicates the formation of TiB_2 and Al_2O_3, along with a small amount of an

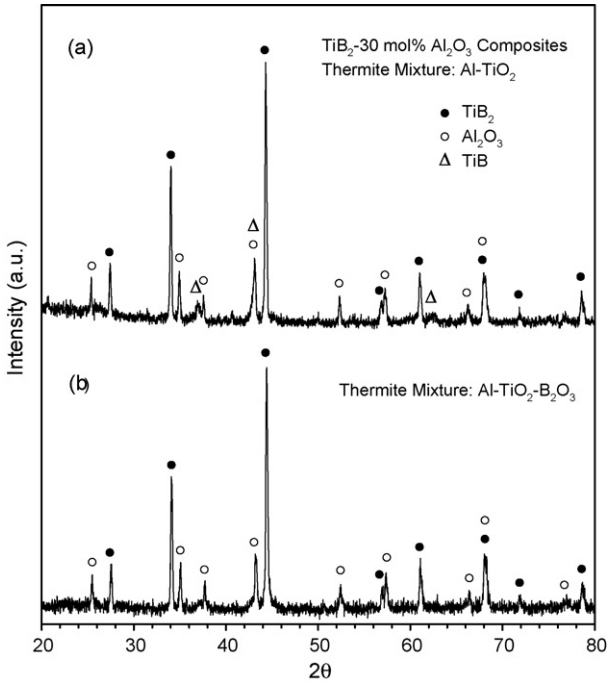

Fig. 8. XRD patterns of TiB_2–30 mol% Al_2O_3 composites produced by SHS involving different thermite mixtures: (a) Al–TiO_2 and (b) Al–TiO_2–B_2O_3.

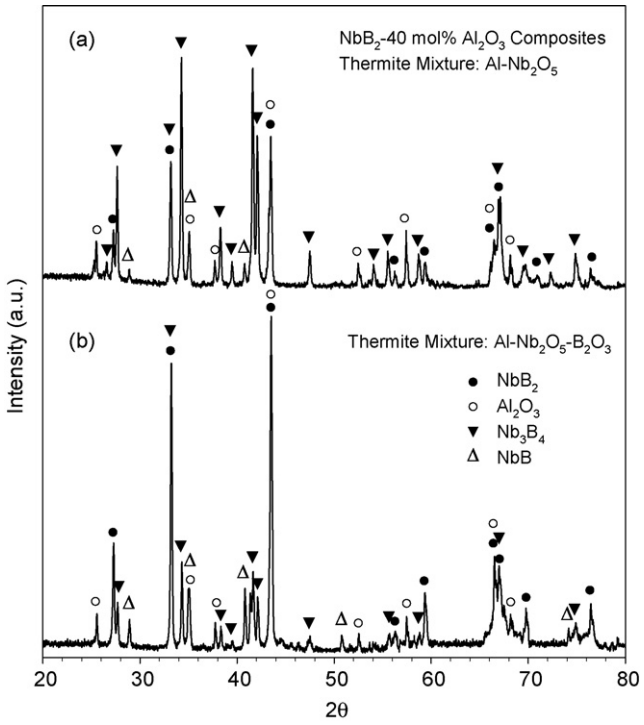

Fig. 9. XRD patterns of NbB_2–40 mol% Al_2O_3 composites produced by SHS involving different thermite mixtures: (a) Al–Nb_2O_5 and (b) Al–Nb_2O_5–B_2O_3.

intermediate boride phase TiB. However, as revealed in Fig. 8b, the TiB phase is almost negligible in the XRD spectrum for the powder compact involving the thermite mixture of Al–TiO_2–B_2O_3. This verifies a better degree of the product formation, due to the presence of B_2O_3 that melts at a low temperature of 450 °C and improves the formation of TiB_2.

For the preparation of the NbB_2–Al_2O_3 composite, Fig. 9a and b shows the existence of three boride phases NbB_2, Nb_3B_4, and NbB in the synthesized products. When compared with that in Fig. 9a using the thermite mixture of Al–Nb_2O_5, Fig. 9b indicates that the relative intensity of the Nb_3B_4 peaks is significantly reduced and NbB_2 is identified as the dominant boride phase for the sample adopting the thermite mixture of Al–Nb_2O_5–B_2O_3. The presence of a large amount of Nb_3B_4 in the final product of Fig. 9a stems most likely from the insufficient reaction time caused by fast propagation of the combustion wave. Therefore, an improvement in the product formation shown in Fig. 9b is attributed to the lower reaction velocity as well as the melting of B_2O_3 in the case of utilizing Al–Nb_2O_5–B_2O_3 as the thermite reactants.

The combustion products feature a highly porous structure and have a relative density of about 40–45%. Typical SEM micrographs, shown in Fig. 10a and b, reveal the grains with a small and rather uniform particle size. This confirms the feasibility of applying the SHS technique to fabricate the soft-agglomerated composite powders with homogeneous distribution of the components. In comparison with conventional methods, the SHS-derived powders eliminate the less efficient mechanical mixing of both components, the prolonged grinding of disagglomeration, and the steps of removal of the impurities [23]. Therefore, the SHS-derived powders enable the simplification of processing ceramic materials by shaping, sintering, and hot-pressing of powders [23].

According to the formation sequence of TiB_2 [24–26] and the XRD results of the synthesized products of this study, the reaction mechanism for the synthesis of the TiB_2–Al_2O_3 composite is proposed as follows. The interaction of Ti with B acts as the first reaction step, which proceeds with formation of TiB and triggers the

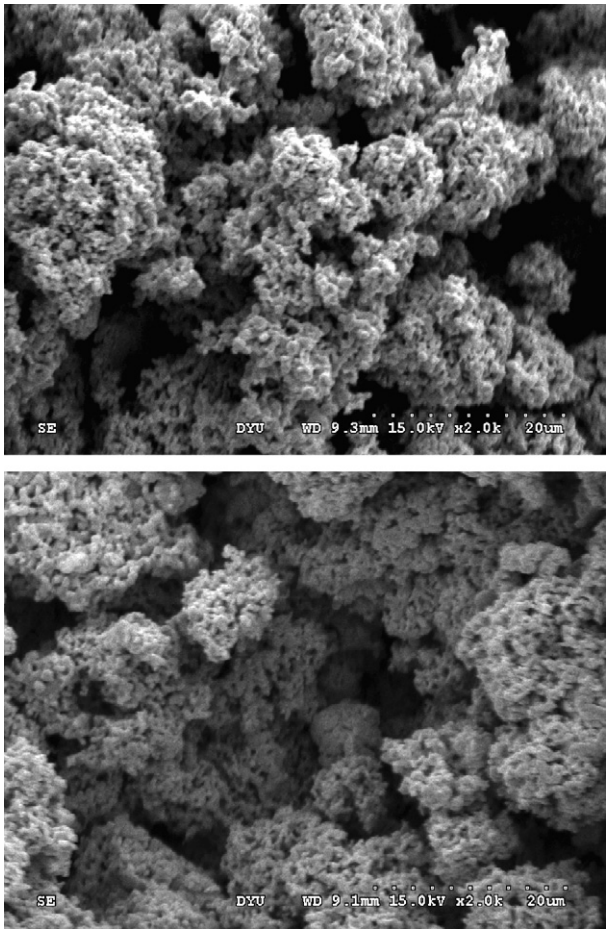

Fig. 10. Typical SEM micrographs of combustion-synthesized products with compositions of (a) TiB_2–30 mol% Al_2O_3 and (b) NbB_2–40 mol% Al_2O_3.

displacement reaction between the thermite reagents. The intermediate boride phase TiB then converts into TiB_2 through further reaction with B. The reaction steps involved in SHS formation of the TiB_2–Al_2O_3 composite are given below.

$$Ti + B \rightarrow TiB \quad (6)$$

$$4Al + 3TiO_2 \rightarrow 3Ti + 2Al_2O_3 \quad (7)$$

$$2Al + B_2O_3 \rightarrow 2B + Al_2O_3 \quad (8)$$

$$TiB + B \rightarrow TiB_2 \quad (9)$$

For the production of the NbB_2–Al_2O_3 composite, however, the SHS process is initiated by the displacement reactions of Al with Nb_2O_5 and B_2O_3. Subsequently, the elemental reaction between Nb and B takes place to generate NbB as an intermediate. Prior to the appearance of NbB_2, the other intermediate boride phase Nb_3B_4 is yielded. The sequence of reaction steps associated with SHS formation of the NbB_2–Al_2O_3 composite is expressed as follows.

$$10Al + 3Nb_2O_5 \rightarrow 6Nb + 5Al_2O_3 \quad (10)$$

$$2Al + B_2O_3 \rightarrow 2B + Al_2O_3 \quad (11)$$

$$Nb + B \rightarrow NbB \quad (12)$$

$$3NbB + B \rightarrow Nb_3B_4 \quad (13)$$

$$Nb_3B_4 + 2B \rightarrow 3NbB_2 \quad (14)$$

4. Conclusions

In this study, the SHS process involving thermite reactions of the different types was conducted to prepare the TiB_2–Al_2O_3 and NbB_2–Al_2O_3 in situ composites. Experimental results indicate that the sustainability of the synthesis reaction, dynamics of the combustion wave, and phase composition of the synthesized product are substantially influenced by the addition of thermite reactions to the elemental SHS process.

In order to produce the TiB_2–Al_2O_3 composites, two thermite mixtures of Al–TiO_2 and Al–TiO_2–B_2O_3 were incorporated with the Ti–B elemental combustion system. Because of the lower exothermicity, the flame-front propagation velocity and combustion temperature were decreased by increasing the extent of the thermite reaction for a higher content of Al_2O_3 formed in the composite. When the thermite mixture of Al–TiO_2–B_2O_3 was used, the melting of B_2O_3 during the SHS process improved the formation of final products. Moreover, the sample compacts containing the thermite mixture of Al–TiO_2–B_2O_3 were shown to yield the TiB_2–Al_2O_3 composite with a broader range of the phase composition up to 62.5 mol% of Al_2O_3, when compared with 35 mol% produced by those involving the thermite mixture of Al–TiO_2.

On formation of NbB_2–Al_2O_3 composites, thermite mixtures of Al–Nb_2O_5 and Al–Nb_2O_5–B_2O_3 were studied. In contrast to the case of preparing the TiB_2–Al_2O_3 composite, addition of the thermite mixtures to the Nb–B elemental combustion system increased the combustion temperature and reaction front velocity. As a result of the greater exothermicity, higher combustion temperatures and flame-front speeds were observed in the powder compacts containing the thermite reactant of Al–Nb_2O_5 than that of Al–Nb_2O_5–B_2O_3. However, the rapid reaction front led to insufficient reaction time for achieving complete formation of the product. Therefore, in addition to Al_2O_3 three boride phases Nb_3B_4, NbB, and NbB_2 were detected in the synthesized products. For the test samples involving the thermite reaction of Al–Nb_2O_5–B_2O_3, the XRD analysis identifies NbB_2 as the major boride phase, rather than Nb_3B_4 which dominates in case of adopting that of Al–Nb_2O_5. The improvement in formation of NbB_2 was mainly attributed to the longer reaction time and the presence of molten B_2O_3 for the SHS process involving the Al–Nb_2O_5–B_2O_3 thermite system.

Acknowledgements

This research was sponsored by the National Science Council of Taiwan, ROC, under the grant of NSC 95-2221-E-212-053-MY2.

References

[1] M. Gu, C. Huang, S. Xiao, H. Liu, Improvements in mechanical properties of TiB_2 ceramics tool materials by dispersion of Al_2O_3 particles, Mater. Sci. Eng. A486 (2008) 167–170.
[2] T. Tsuchida, T. Kakuta, MA-SHS of NbC and NbB_2 in air from the Nb/B/C powder mixtures, J. Eur. Ceram. Soc. 27 (2007) 527–530.
[3] S.K. Mishra, S.K. Das, L.C. Pathak, Sintering behavior of self-propagating high temperature synthesized ZrB_2–Al_2O_3 composite powder, Mater. Sci. Eng. A426 (2006) 229–234.
[4] S.K. Mishra, S.K. Das, V. Sherbacov, Fabrication of Al_2O_3–ZrB_2 in situ composite by SHS dynamic compaction: a novel approach, Composit. Sci. Technol. 67 (2007) 2447–2453.
[5] A.R. Keller, M. Zhou, Effect of microstructure on dynamic failure resistance of titanium diboride/alumina ceramics, J. Am. Ceram. Soc. 86 (3) (2003) 449–457.
[6] Z.A. Munir, U. Anselmi-Tamburini, Self-propagating exothermic reactions: the synthesis of high-temperature materials by combustion, Mater. Sci. Rep. 3 (1989) 277–365.
[7] A.G. Merzhanov, Solid flames: discoveries, concepts, and horizons of cognition, Combust. Sci. Technol. 98 (1994) 307–336.
[8] A. Varma, J.P. Lebrat, Combustion synthesis of advanced materials, Chem. Eng. Sci. 47 (1992) 2179–2194.
[9] J.J. Moore, H.J. Feng, Combustion synthesis of advanced materials: part I. reaction parameters, Prog. Mater. Sci. 39 (1995) 243–273.
[10] L.L. Wang, Z.A. Munir, Y.M. Maximov, Thermite reactions: their utilization in the synthesis and processing of materials, J. Mater. Sci. 28 (1993) 3693–3708.

[11] M.A. Meyers, E.A. Olevsky, J. Ma, M. Jamet, Combustion synthesis/densification of an Al_2O_3–TiB_2 composite, Mater. Sci. Eng. A311 (2001) 83–99.
[12] C.L. Yeh, R.F. Li, Formation of TiAl–Ti_5Si_3 and TiAl–Al_2O_3 in situ composites by combustion synthesis, Intermetallics 16 (2008) 64–70.
[13] M.J. Mas-Guindal, E. Benko, M.A. Rodríguez, Nanostructured metastable cermets of Ti–Al_2O_3 through activated SHS reaction, J. Alloys Compd. 454 (2008) 352–358.
[14] D. Vallauri, V.A. Shcherbakov, A.V. Khitev, F.A. Deorsola, Study of structure formation in TiC–TiB_2–Me_xO_y ceramics fabricated by SHS and densification, Acta Mater. 56 (2008) 1380–1389.
[15] Q. Hu, P. Luo, Y. Yan, Microstructures, densification and mechanical properties of TiC–Al_2O_3–Al composite by field-activated combustion synthesis, Mater. Sci. Eng. A486 (2008) 215–221.
[16] Y.H. Liang, H.Y. Wang, Y.F. Yang, R.Y. Zhao, Q.C. Jiang, Effect of Cu content on the reaction behaviors of self-propagating high-temperature synthesis in Cu–Ti–B_4C system, J. Alloys Compd. 462 (2008) 113–118.
[17] P. Shen, B. Zou, S. Jin, Q. Jiang, Reaction mechanism in self-propagating high temperature synthesis of TiC–TiB_2/Al composites from an Al–Ti–B_4C system, Mater. Sci. Eng. A 454–455 (2007) 300–309.
[18] M. Binnewies, E. Milke, Thermochemical Data of Elements and Compounds, Wiley-VCH, Weinheim, New York, 1999.
[19] C.L. Yeh, W.Y. Sung, Synthesis of NiTi intermetallics by self-propagating combustion, J. Alloys Comp. 376 (2004) 79–88.
[20] C.L. Yeh, H.C. Chuang, Experimental studies on self-propagating combustion synthesis of niobium nitride, Ceram. Int. 30 (5) (2004) 733–743.
[21] K. Morsi, Review: reaction synthesis processing of Ni–Al intermetallic materials, Mater. Sci. Eng. A299 (2001) 1–15.
[22] D.E. Alman, Reactive sintering of TiAl–Ti_5Si_3 in situ composites, Intermetallics 13 (2005) 572–579.
[23] R. Pampuch, Some fundamental versus practical aspects of self propagating high-temperature synthesis, Solid State Ionics 101–203 (1997) 899–907.
[24] D. Vallauri, I.C. AtíasAdrián, A. Chrysanthou, TiC–TiB_2 composites: a review of phase relationships, processing and properties, J. Eur. Ceram. Soc. 28 (2008) 1697–1713.
[25] A.M. Locci, R. Orrŭ, G. Cao, Z.A. Munir, Simultaneous spark plasma synthesis and densification of TiC–TiB_2 composites, J. Am. Ceram. Soc. 89 (2006) 848–855.
[26] H. Zhao, Y.B. Cheng, Formation of TiB_2–TiC composites by reactive sintering, Ceram. Int. 25 (1999) 353–358.